J Toxicol Pathol 2004; 17: 113–118

Original

Hypospadias and Incomplete Preputial Separation in Male Rats Induced by Prenatal Exposure to an Anti-androgen, Flutamide

Shinsuke Yoshimura[1], Hajime Yamaguchi[1], Kazunori Konno[1], Noriko Ohsawa[1], Satoshi Noguchi[1], and Akiko Chisaka[1]

[1]Hatano Research Institute, Food and Drug Safety Center, 729–5, Ochiai, Hadano, Kanagawa 257–8523, Japan

Abstract: Hypospadias was induced in male Sprague-Dawley rats by prenatal exposure to 30 mg/kg/day of flutamide from gestational days 14 to 17, or from 18 to 21. Their external genitalia were examined histopathologically and compared to untreated controls. On postnatal day 6, the glans penis of untreated controls was bordered with epithelium. On postnatal day 22, papillae were recognized on the glans penis side, and cornification started close to the tip of the papilla on postnatal day 35. On postnatal day 42 cornification spread to the surface of the glans penis. The cornification progressed from tip to base of the glans penis, and from dorsal to ventral. When cornification reached the base of the glans penis, separation of the double layered epithelia was complete and the animal was considered sexually mature. Flutamide treatment on gestational days 14–17 induced a defect in the ventral half of the glans penis (cleft phallus) and cleft in the ventral prepuce (cleft prepuce) in the male pups, while treatment on gestational days 18–21 induced cleft phallus without apparent abnormalities in the prepuce. The external urethral orifice opened at the ventral end of the glans penis (hypospadias) in both treatment groups. In male pups with cleft phallus, cornification of the dorsal epithelium followed by separation of the prepuce occurred, while separation of the ventral part of glans penis did not occur because epithelium was not formed at the ventral part of the glans penis. Consequently, the onset of puberty was not decided in these animals. These findings indicate that the defect of the ventral half of the phallus is the reason why the time of sexual maturation was not decided, and that there is a difference between the phallus and prepuce in the sensitive period concerning the development of flutamide-induced malformations.
(J Toxicol Pathol 2004; **17**: 113–118)

Key words: flutamide, anti-androgen, rat, prenatal exposure, hypospadias

Introduction

Preputial separation, which is observed as separation of the prepuce from the glans penis, has been used as a sign of puberty in the male rat. Histological observation on the progress of preputial separation after cornification at the lining of prepuce and surface of glans penis was well described using Long-Evans rats in 1942[1]. Preputial separation is thought to be dependent on androgens, because castration blocked preputial separation, and the addition of testosterone (TS) or dihydrotestosterone (DHT) recovered the effect of castration[1,2]. In recent years, preputial separation has been used as an endpoint to evaluate endocrine disrupting chemicals. Although the observation of preputial separation is a useful tool for detecting sexual maturation, anti-androgenic chemicals induce hypospadias in male rats by intrauterine exposure. The time of sexual maturation is determined by complete separation of the prepuce from the ventral surface of the glans penis, but in males with hypospadias, puberty is undetermined because this complete separation in the glans penis is not evident[3].

The purpose of this study was to reveal the histological process of normal and abnormal preputial separation, as well to reveal the reason why the time of sexual maturation cannot be decided in males with hypospadias induced by prenatal exposure to flutamide (FLU), an anti-androgenic chemical, in Sprague-Dawley rats. FLU was administered on gestational days (GD) 14–17 (expected to be the most sensitive period for hypospadias) or on GD 18–21 (thought to be a less sensitive period for hypospadias).

Materials and Methods

Sprague-Dawley rats (Crj:CD (SD) IGS), 30 males and 33 females, 11 weeks of age, were obtained from Charles

Received: 26 January 2004, Accepted: 15 April 2004
Mailing address: Shinsuke Yoshimura, Laboratory of Toxicology, Hatano Research Institute, Food and Drug Safety Center, 729–5, Ochiai, Hadano, Kanagawa 257–8523, Japan
TEL: 81-463-82-4751 FAX: 81-463-82-9627
E-mail: yoshimura.s@fdsc.or.jp

River Japan, Inc. (Atsugi, Japan). All animals were acclimatized to laboratory conditions and quarantined for one week before mating. Rats used for this study were selected based upon general condition, appearance and behavior during the acclimatization period. Animals were housed individually in wire-bottom metal cages (220 × 270 × 190 mm) and kept in a barrier sustained animal room that was maintained at 21.0 – 25.0°C and 40.0 – 75.0% relative humidity with a 12-hour artificial light cycle (lighting from 7:00 to 19:00). Fifteen changes of room air per hour were provided. Commercial diet CE-2 (CLEA Japan, Inc., Tokyo) and water (Hadano City) were available ad libitum throughout the study. The protocol of the present study was approved by the Animal Use Committee of the Hatano Research Institute.

The untreated control group consisted of 18 females. While the second group, consisting of 9 females, was treated orally with 30 mg/kg/day of FLU (Sigma Chemical Co., St. Louis, USA) dissolved in corn oil (Nacalai Tesque, Inc., Kyoto, Japan) from GD 14 to 17, the third group, consisting of 6 females, was treated with the same dose from GD 18 to 21. From the result of a preliminary study the dosage was decided as 30 mg/kg/day, because pregnant rats died after administration of 100 mg/kg/day of FLU. To obtain pregnant animals, 12-week-old females were cohabited overnight on a 1:1 basis with males 12 weeks of age or older. Females were considered to be at GD 0 when daily examination revealed a vaginal plug. All pregnant animals were housed in cages with animal bedding (PAPER CLEAN®, Japan SLC, Inc., Shizuoka) from GD 18 until postpartum day 10, and allowed to give birth. On postnatal day (PND) 6 (PND 0 is the day of delivery) all female pups were discarded. Body weights of male pups were measured on PND 0, 6, 22, 35 and 56. Progress of preputial separation of male pups was observed macroscopically from PND 35.

Control male pups were sacrificed by exsanguination under anesthesia on PND 6, 22, 35, 42 and 56 (number of pups in group 1 were 6, 16, 15, 4 and 24, respectively). Male pups from FLU-treated females were sacrificed under anesthesia on PND 6 and 56 (number of pups in group 2 were 18 and 41, respectively, and those in group 3 were 8 and 21, respectively). After macroscopic examination, the prepuce and penis were dissected and fixed with 0.1 mol/L phosphate buffered 10% formalin solution. Sagittal slices of the prepuce and penis were embedded in paraffin, and sections were stained with hematoxylin-eosin (H & E) for histopathological examination.

Results

On macroscopic examination, the glans penis of control males was covered with prepuce, and the prepuce could be completely retracted to expose the glans penis until PND 46 (Figs. 1A, 1B). Prepuce of males prenatally exposed to FLU on GD 14–17 had a cleft at the ventral part (cleft prepuce), and the glans penis was observed from the cleft (Fig. 1C). The ventral part of the glans penis of these males was incompletely formed (cleft phallus) and the os penis was often exposed (Fig. 1D). The incidence of cleft prepuce was 80% (33/41), and the incidence of cleft phallus was 90% (37/41). Cleft prepuce is usually observed with cleft phallus. Another 4 males showed no cleft on their prepuce or phallus, while preputial separation was delayed or incomplete on PND 56. Although there was no cleft at the prepuce of males exposed to FLU on GD 18–21 (Fig. 1E), the ventral part of the glans penis was incompletely formed (cleft phallus, Fig. 1F), and incidence of the cleft phallus in this group was 100% (21/21). Body weight gains of males were not affected by FLU exposure.

Upon histological examination of untreated controls on PND 6, the glans penis was bordered with specific epithelium (Fig. 2A). The epithelium consisted of outer and inner basal layers (Fig. 2B). The outer layer lined the inside of the prepuce and the inner layer covered the glans penis. The urethra was located in the center of the glans penis and the os penis was observed between the dorsal surface of the glans penis and the urethra (Fig. 2A). On PND 22, there were many papillary processes from the glans penis (arrows in Fig. 2C), and the surface of these processes was covered with squamous epithelial cells. At this point the two basal layers lost their parallel arrangement. On PND 35, the epithelial layer consisted of stratified squamous epithelium, and the surface of the papillary processes (arrows in Fig. 2D) was covered with cornified cells. The cornified layer was limited to the surface of these processes. On PND 42, epithelial cells between the papillae also cornified, and both surfaces of the penis and prepuce consisted of keratinized stratified squamous epithelium. Cornification and separation were incomplete at the basal part of the glans penis. Separation at the ventral surface of the glans penis was more delayed than that at the dorsal surface. On PND 56 cornification was complete from the tip to the base of the glans penis and the ventral surface also showed cornified layers (Figs. 2E, 2F). The preputial separation was complete across the entire surface of the glans penis.

Histological examination of males prenatally exposed to FLU on GD 14–17 revealed a cleft at the ventral surface of genital tubercle on PND 6 (arrow in Fig. 3A). The urethra was not located in the center of the glans penis, but instead was observed at the ventral surface of the glans penis. The dorsal part of the glans penis was bordered by epithelium as observed in controls, while the ventral part was covered with urethral epithelium. This finding indicates that the ventral half of glans penis was not formed (comparison with controls as shown by an asterisk (*) in Fig. 2A). The cavernous body of the penis was tortuous and also observed in PND 56 males exposed to FLU on GD 14–17 (Fig. 3B). The dorsal surface of the glans penis and prepuce of PND 56 males were covered with keratinized stratified squamous epithelium, and the prepuce was separated from the glans penis (Fig. 3B). The ventral part of the glans penis and ventral epithelium were not formed between the urethra and subcutis, the ventral surface of the glans penis was not covered with squamous epithelium and the preputial

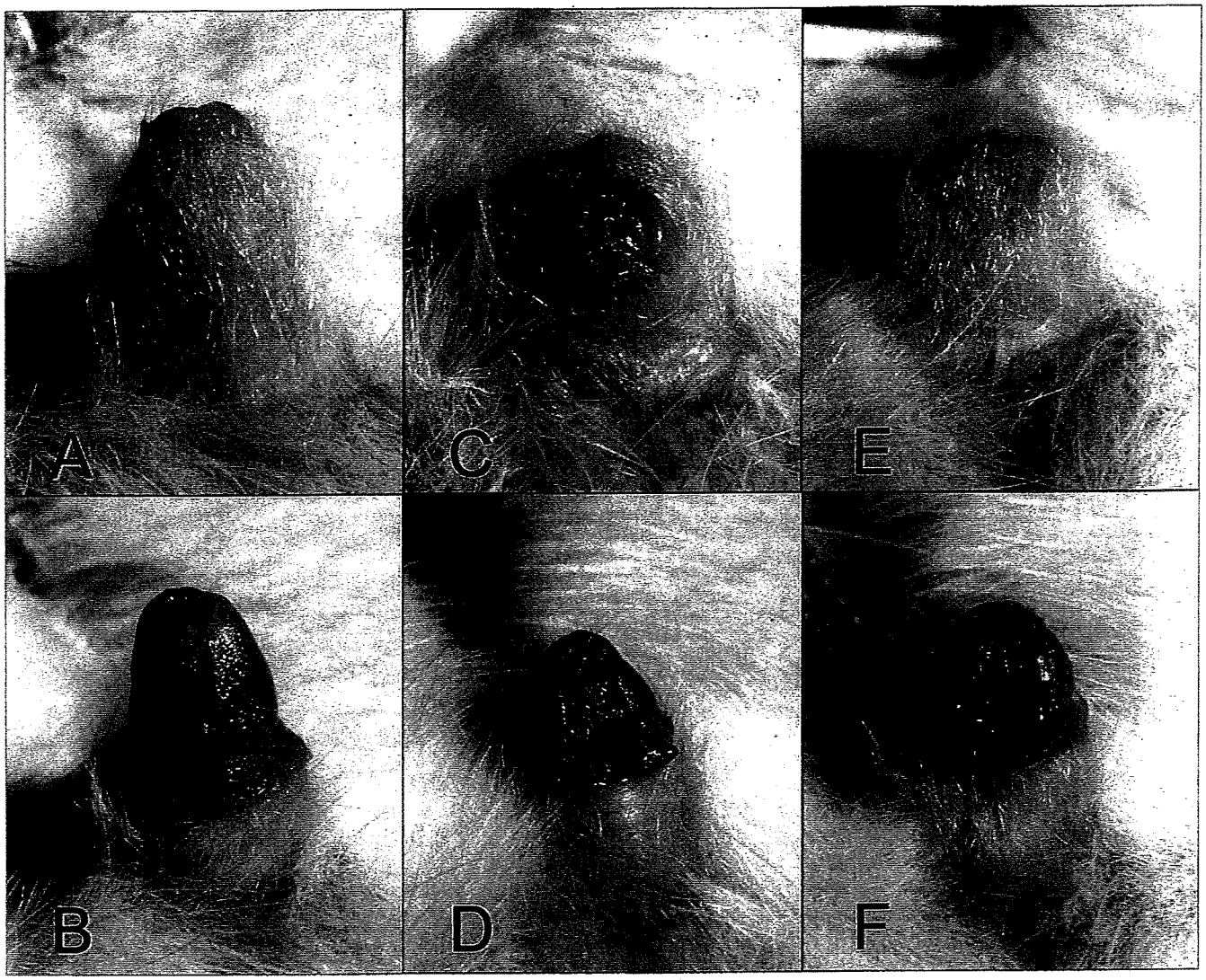

Fig. 1. Ventral surface of genital tubercle (A, C and E) and glans penis (B, D and F) of males at PND 56. A and B: Control rat. Prepuce is completely retracted. C and D: Male rat prenatally exposed to FLU on GD 14–17. Ventral side of the prepuce has a cleft, and the glans penis is observed from the cleft. Ventral part of the glans penis is incompletely formed (cleft phallus) and os penis is observed. E and F: Male rat prenatally exposed to FLU on GD 18–21. Prepuce does not have a cleft at the ventral side. Glans penis shows cleft phallus and os penis is observed.

separation did not progress at the ventral part. The external urethral orifice opened at the ventral surface of the glans penis (hypospadias). The preputial tissue was hypoplastic and the tip of the penis was not overlain with prepuce.

The glans penis of PND 6 males exposed to FLU on GD 18–21 was covered with skin, and a cleft was not observed at the ventral part of genital tubercle (Fig. 3C). The dorsal part of the glans penis was bordered by epithelium, but the ventral part of the glans penis and ventral epithelium were not formed between the urethra and subcutis (comparison with controls as shown by an asterisk (*) in Fig. 2A). The tortuous structure of the cavernous body was indistinct. The prepuce overlaid the glans penis of PND 56 males exposed on GD 18–21 (Fig. 3D). The dorsal surface of the glans penis of these males was covered with keratinized stratified squamous epithelium, and the prepuce was separated from the glans penis. The ventral part of the glans penis and ventral epithelium were not formed between the urethra and subcutis, and preputial separation did not progress at the ventral part. In these rats the external urethral orifice opened at the ventral surface of the glans penis.

Discussion

As described above, preputial separation in untreated rats initiated from cornification of the epithelium on the penile side lying in the dual phasic epithelium between the glans penis and prepuce. Cornification began at the surface very close to the apex of the papillary process from the glans penis, and when the cornification reached the next papilla the prepuce separated from the glans penis. Preputial separation progressed from the tip of the glans penis towards its base,

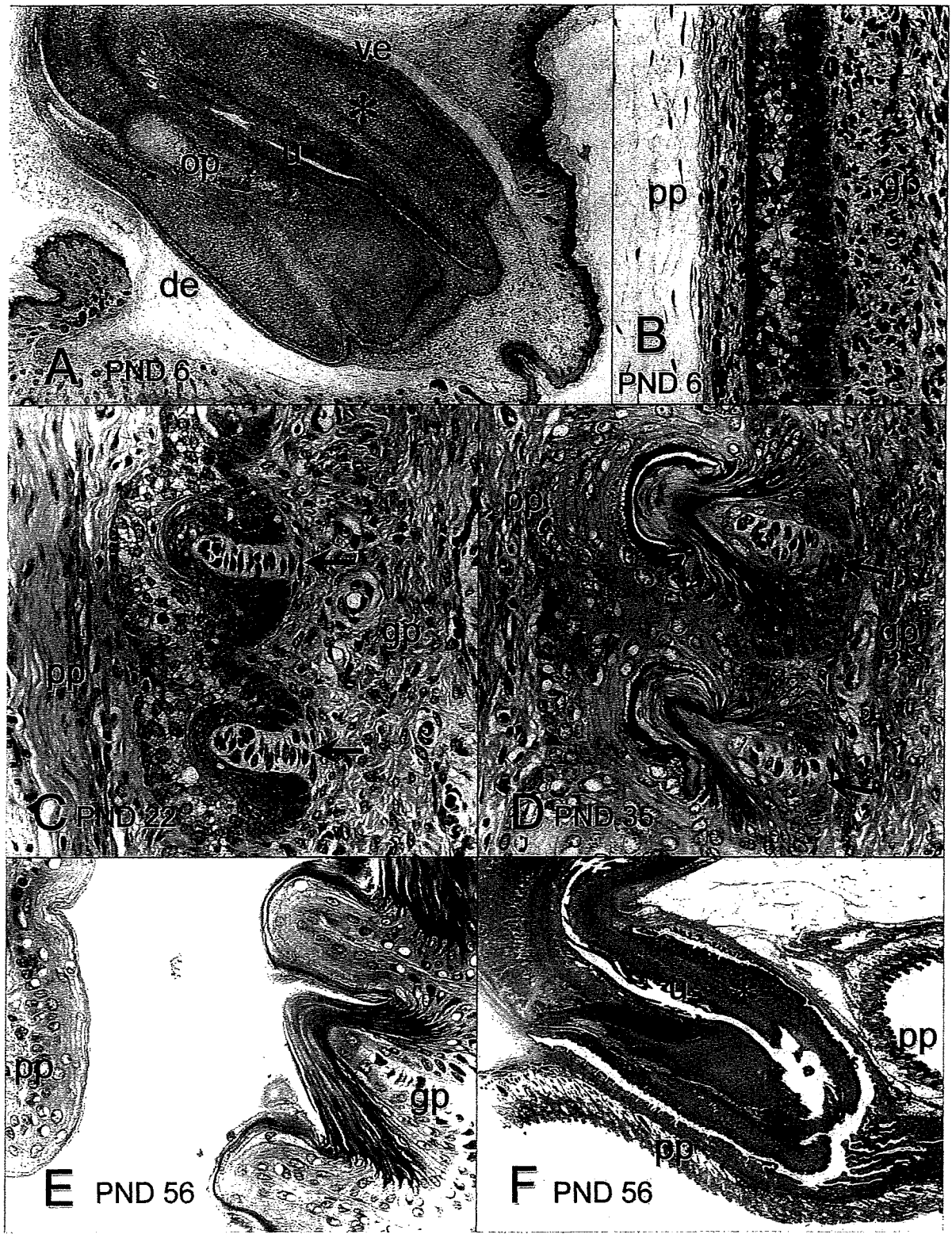

Fig. 2. Sagittal sections of the genital tubercle from control males.
A: Genital tubercle of a male on PND 6. Glans penis is bordered with dorsal epithelium (de) and ventral epithelium (ve). Urethra (u) is located in the center of the glans penis. op: os penis. *: ventral half of the glans penis.
B, C, D and E: Epithelium between the dorsal part of the glans penis (gp) and prepuce (pp) on PND 6, 22, 35 and 56, respectively. Epithelium of PND 6 consisted of outer and inner basal layers (B). Squamous epithelial cell of PND 22 is covering the papillary processes (arrows) from the glans penis (C). Epithelial layer of PND 35 consists of stratified squamous epithelium, and cornified layer is covering the papillary processes (arrows in D). Whole surface of both the glans penis and prepuce is covered with cornified layer on PND 56 (E).
F: Glans penis and prepuce on PND 56. Preputial separation is completed. Urethra (u) is located in the center of the glans penis.
*: ventral half of the glans penis. H & E. Magnification, A: × 35, B, C and D: × 400, E: × 330, F: × 9.

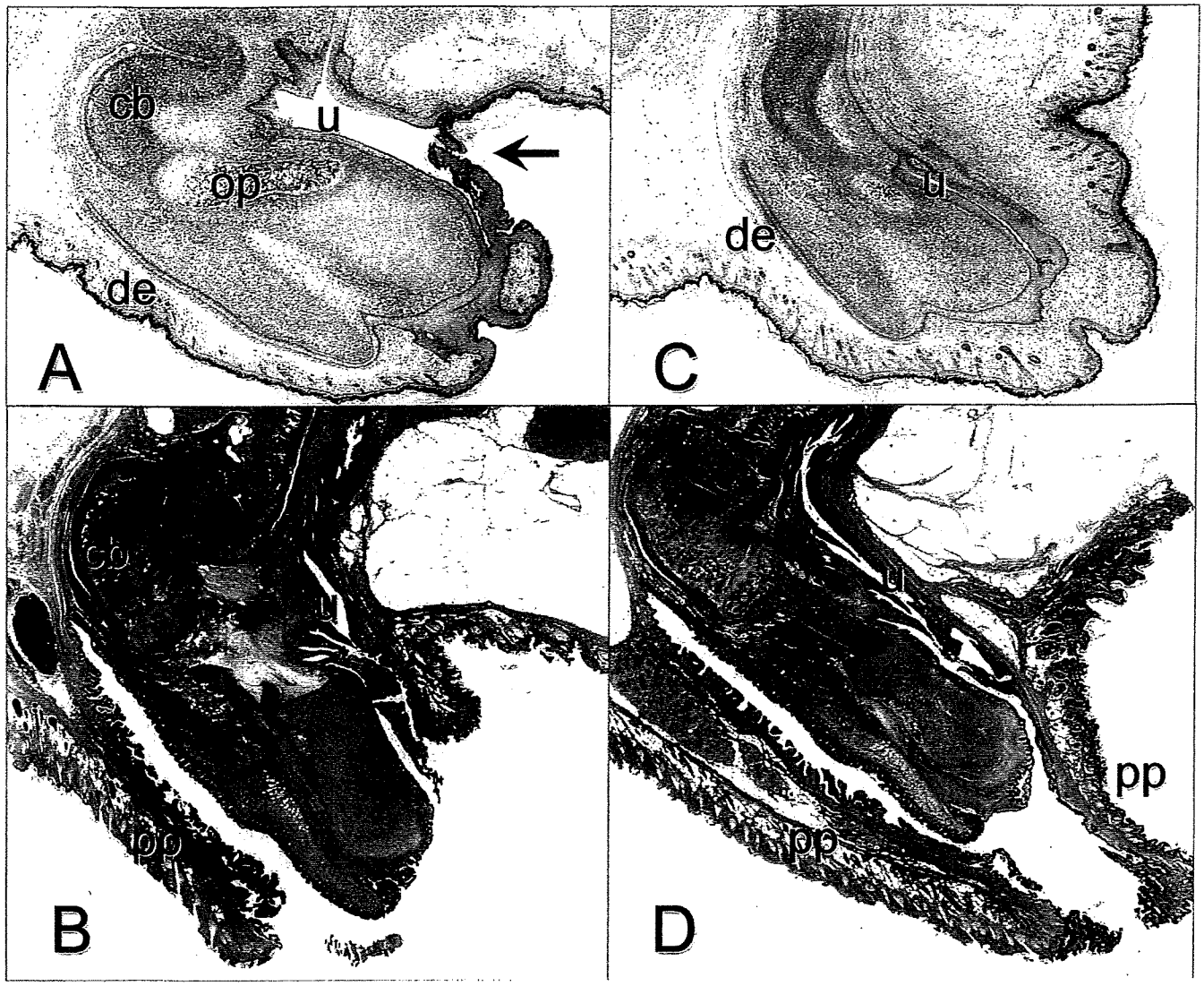

Fig. 3. Sagittal sections of genital tubercle from males prenatally exposed to FLU on GD 14–17 (A, B) or GD 18–21 (C, D), sacrificed on PND 6 (A, C) and PND 56 (B, D).
A: There is a cleft (arrow in the figure) at the ventral side of genital tubercle. Urethra (u) is observed at the ventral surface of the glans penis. Dorsal part of the glans penis is bordered with epithelium (de). Cavernous body (cb) shows tortuous structure.
B: Prepuce (pp) is separated from the glans penis at the dorsal part. Prepuce is hypoplastic, and the glans penis is not completely overlain with the prepuce. Urethra is located between the glans penis and subcutis.
C: Cleft is not formed at the ventral side of genital tubercle. Dorsal part of the glans penis is bordered with epithelium (de). Ventral part of the glans penis and ventral epithelium is not formed. Urethra is located between the glans penis and subcutis.
D: Prepuce is separated from the glans penis at the dorsal part. The ventral part of the glans penis and ventral epithelial layer is not formed. The glans penis is completely overlain with the prepuce.
H&E. Magnification, A and C: × 27; B and D: × 10.

and also from the dorsal to ventral surface of the glans penis. Histological features observed in controls of this study were almost the same as shown in Long-Evans rats[1]. Complete separation was not observed in animals exposed to FLU in their fetal period, since they had a cleft phallus at their ventral surface of the glans penis. Histopathological examination revealed defects in the ventral part of the glans penis and lack of an epithelial layer at the ventral part in newborn rats.

Induction of hypospadias has been reportedly caused by various chemicals, which include anti-androgens such as FLU, vinclozolin and finasteride. FLU is a well-known potent androgen receptor antagonist and is used as a nonsteroidal anti-androgen drug for the treatment of prostate cancer. FLU inhibits TS and DHT binding to the intracellular androgen receptor and prenatal/perinatal exposure to FLU induces abnormalities in the genital tract such as hypospadias, agenesis of the prostate, epididymis and vas deferens[2,4,5]. Vinclozolin, a fungicide, is also an androgen receptor antagonist, and induces hypospadias in

rats by perinatal (GD 14 to day 3 postpartum)[6] or prenatal (for 2 days in GD 12–21)[7] administration. Finasteride, which inhibits 5α-reductase conversion of TS to DHT, also induces hypospadias in male rats exposed from GD 15 to day 21 postpartum, and based on this finding DHT is thought to be involved in the development of external genitalia[8]. While the Wolffian ducts are dependent on TS, their derivatives such as the epididymis, vas deferens or seminal vesicles were not affected by intrauterine exposure to finasteride[8]. Hypoplastic change in the genital tubercle was reported in fetuses exposed to finasteride from GD 6 to 20[9]. Wedge shaped mesenchymal tissue between rectum and urogenital sinus failed to develop in these fetuses, and the urethra opened near the base of the tubercle. This finding indicates that the mesenchymal wedge may be the most sensitive area to loss of the effect of DHT in male fetuses. Our study also revealed a defect in the ventral part of the glans penis, in which preputial separation could not progress, and this is the reason why the time of sexual maturation could not be decided in males with hypospadias.

Androgen receptors are detectable in the mesenchymal cells of the rat urogenital tubercle from fetal day 14 onwards[10]. In many studies of sexual differentiation and male reproductive organ malformation, dosing starts from GD 12 or 14. The most sensitive period to induce hypospadias is reportedly GD 15–16 with 400 mg/kg of vinclozolin exposure, and the incidence was 42% (10/24), while only weak sensitivity (11%, 1/9) was found with treatment on GD 17–18[7]. Similar results were obtained in our study of vinclozolin (unpublished data)[11]. Exposure to 100 mg/kg of vinclozolin on GD 14–17 induced cleft phallus with cleft prepuce, and the incidence was 85%, but exposure on GD 18–21 induced no abnormalities in external genitalia. Pregnant females or newborn pups died after exposure to 200 mg/kg of vinclozolin. Finasteride exposed rats also showed similar results[8]. Male pups exposed to 20 mg/kg of finasteride on GD 16–17 showed hypospadias, and the incidence was 39% (14/36), while incidence in the GD 18–19 group was 0% (0/36).

Many reports describe the malformation of the phallus as hypospadias, but details and the incidence of the prepuce malformations are not clear. In our study, pregnant rats were administered with 30 mg/kg of FLU on GD 14–17, which was considered to be the sensitive period, and the incidence of cleft phallus and cleft prepuce was compared to the exposure on GD 18–21. Male pups exposed to FLU on GD 14–17 showed cleft phallus with hypospadias (90%) and cleft prepuce (80%), while males exposed on GD 18–21 had cleft phallus with hypospadias (100%) without apparent abnormality in the prepuce. A lower dose of FLU also showed similar results with lower incidence (unpublished data)[11]. Exposure of 10 mg/kg of FLU on GD 14–17 induced cleft phallus (58%) and cleft prepuce (25%), while exposure on GD 18–21 induced cleft phallus (25%) without apparent abnormality in the prepuce. These findings show that the period of sensitivity to FLU in terms of phallus malformation is different from vinclozolin and finasteride, and also that there are differences among the sensitive periods between the phallus and prepuce concerning FLU-induced malformations.

Acknowledgments: This work was supported by Health and Labour Sciences Research Grants from the Ministry of Health, Labour and Welfare of Japan. We would also like to thank Dr. Masayoshi Kanisawa for proofreading this manuscript.

References

1. Lyons WR, Berlin I, and Friedlander S. Cornification of balano-preputial epithelium in normal rats and in castrated rats treated with testosterone propionate. Endocrinology 1942; **31**: 659–663.
2. Korenbrot CC, Huhtaniemi IT, and Weiner RI. Preputial separation as an external sign of pubertal development in the male rat. Biol Reprod 1977; **17**: 298–303.
3. McIntyre BS, Barlow NJ, and Foster PMD. Androgen-mediated development in male rat offspring exposed to flutamide *in utero*: permanence and correlation of early postnatal changes in anogenital distance and nipple retention with malformations in androgen-dependent tissues. Toxicol Sci 2001; **62**: 236–249.
4. Mylchreest E, Sar M, Cattley RC, and Foster PMD. Disruption of androgen-regulated male reproductive development by di(*n*-butyl) phthalate during late gestation in rats is different from flutamide. Toxicol Appl Pharmacol 1999; **156**: 81–95.
5. Miyata K, Yabushita S, Sukata T, Sano M, Yoshino H, Nakanishi T, Okuno Y, and Matsuo M. Effects of perinatal exposure to flutamide on sex hormones and androgen-dependent organs in F1 male rats. J Toxicol Sci 2002; **27**: 19–33.
6. Gray LE Jr, Ostby JS, and Kelce WR. Developmental effects of an environmental antiandrogen: the fungicide vinclozolin alters sex differentiation of the male rat. Toxicol Appl Pharmacol 1994; **129**: 46–52.
7. Wolf CJ, LeBlanc GA, Ostby JS, and Gray LE Jr. Characterization of the period of sensitivity of fetal male sexual development to vinclozolin. Toxicol Sci 2000; **55**: 152–161.
8. Clark RL, Anderson CA, Prahalada S, Robertson RT, Lochry EA, Leonard YM, Stevens JL, and Hoberman AM. Critical developmental periods for effects on male rat genitalia induced by finasteride, a 5α-reductase inhibitor. Toxicol Appl Pharmacol 1993; **119**: 34–40.
9. Anderson CA and Clark RL. External genitalia of the rat: normal development and the histogenesis of 5α-reductase inhibitor-induced abnormalities. Teratology 1990; **42**: 483–496.
10. Bentvelsen FM, Brinkmann AO, van der Schoot P, van der Linden JETM, van der Kwast TH, Boersma WJA, Schröder FH, and Nijman JM. Developmental pattern and regulation by androgens of androgen receptor expression in the urogenital tract of the rat. Mol Cell Endocrinol 1995; **113**: 245–253.
11. Yoshimura S. Effects of prenatal or postnatal exposure to chemicals on preputial separation of male rats (unpublished).

J Toxicol Pathol 2005; 18: 41–46

Original

Electron Microscopical Evidence of the Protective Function of Thioredoxin (TRX/ADF) Transgene against 2,3,7,8-tetrachlorodibenzo-*p*-dioxin (TCDD)-induced Cellular Toxicity in the Liver and Brain

Byung-Il Yoon[1,5], Toyozo Kaneko[1], Yoko Hirabayashi[1], Takayoshi Imazawa[2], Akiyoshi Nishikawa[2], Yukio Kodama[1], Jun Kanno[1], Junji Yodoi[4], Jeong-Hee Han[5], Masao Hirose[2], and Tohru Inoue[3]

[1]Division of Cellular and Molecular Toxicology
[2]Department of Pathology
[3]Safety and Research Center of National Institute of Health Sciences, Tokyo 158–8501, Japan
[4]Department of Biological Responses, Institute for Virus Research, Kyoto University, Kyoto, Japan
[5]Department of Veterinary Medicine, Kangwon National University, Chunchcon 200–701, Korea

Abstract: The present study was performed to assess the protective role of thioredoxin/adult T-cell leukemia-derived factor (TRX/ADF) on the liver and brain cell damages induced by 2,3,7,8-tetrachlorodibenzo-*p*-dioxin (TCDD) in ADF wild-type (WT) and transgenic (Tg) mice. The ADF WT and Tg mice were intraperitoneally injected with a single dose of TCDD (150 μg/kg body weight). One day after the treatment, the liver and brain tissues were examined electron microscopically to evaluate the cellular toxicity. In the ADF WT mice, marked reduction of subcellular components, such as mitochondria, rough endoplasmic reticula, and glycogen granules, as well as swelling of the remaining mitochondria, were evident in the liver cells. However, attenuation of these changes was evident in TCDD-treated TRX/ADF mice. Similar subcellular changes noted in the neuronal cells of TCDD-treated WT mice were also attenuated in Tg mice. The results suggest that oxidative cellular damage contributes to the acute toxicity induced by TCDD and that TRX/ADF protects against it. (J Toxicol Pathol 2005; **18**: 41–46)

Key words: Ah receptor, brain, liver, 2,3,7,8-tetrachlrodibenzo-*p*-dioxin (TCDD), thioredoxin/adult T-cell leukemia-derived factor (TRX/ADF), transgenic (Tg) mouse

Introduction

As one of the aromatic hydrocarbons, 2,3,7,8-tetrachlorodibenzo-*p*-dioxin (TCDD) is a widely spread environmental pollutant that has a broad spectrum of toxic effects on a variety of tissues such as the thymus, liver, testes and central nervous system in mammals[1–6]. Although a number of studies have shown that the toxic effects of TCDD are mediated by intracytoplasmic aromatic hydrocarbon receptor (AhR)[7–9], the toxic mechanism of TCDD on the target organs is still not fully understood. Among the toxic events, oxidative stress is considered to play a major role in the toxic mechanism of TCDD, as characterized by marked increases of lipid peroxidation, the formation of reactive oxygen species, and DNA single-strand break[9–14].

Exogenous xenobiotics, such as aromatic hydrocarbons, result in profound induction of cytochrome P450 enzymes in the liver, resulting in the generation of reactive oxygen species[15,16]. On the other hand, the brain is rich in peroxidizable fatty acids and has relatively low catalase activity[17]. Therefore, these organs are considered to be highly susceptible to oxidative stresses[18]. In fact, the contribution of oxidative stress in TCDD-induced cellular damage of the liver and brain has been suggested in previous studies[13,18–22].

Adult T-cell leukemia-derived factor (ADF) is a human thioredoxin (TRX) associated with the reduction/oxidation (redox) regulation of the cellular environment[23]. TRX/ADF is a stress-inducible protein and its expression is up-regulated after viral infection as well as in cellular stress conditions induced by oxidative agents such as hydrogen peroxide or diamide, irradiation with X-rays and ultraviolet

Received: 24 September 2004, Accepted: 15 February 2005
Mailing address: Byung-Il Yoon, Department of Veterinary Medicine, College of Animal Resources Sciences, Kangwon National University, 192–1 Hyoja2-dong, Chunchcon, Kangwon 200–701, Republic of Korea
TEL: 82-33-250-8679 FAX: 82-33-244-2367
E-mail: byoon@kangwon.ac.kr

light, or ischemic reperfusion[23]. Previous studies have shown that TRX/ADF plays a role in the cellular defense mechanism against oxidative cellular damage via the regulation of intracellular redox status, since exogenously administered TRX/ADF protected cells from oxidative cellular injury[24,25].

We recently reported for the first time the protective function of TRX/ADF against TCDD-induced hematotoxicity in ADF transgenic (Tg) mice, indicating oxidative stress contributes to the hematotoxic mechanism of TCDD[26]. We hypothesized in the present study that overexpression of TRX/ADF might also be effective for protection against the toxic effects of TCDD on the liver and brain tissues in which oxidative stress has also been implicated in the toxic mechanism. For this purpose, we injected TCDD with a dosage capable of inducing oxidative stress in the liver following acute exposure[21], to ADF wild-type (WT) and transgenic (Tg) mice, and then compared subcellular changes electron microscopically in the liver and brain tissues.

Materials and Methods

Animals

TRX/ADF overexpressed mice (ADF Tg mice), originally produced by Dr. A. Mitsui[27], were maintained in a laboratory facility with a 12:12-hour light-dark cycle at an ambient temperature of 21 ± 2°C at the National Institute of Health Sciences (NIHS) of Japan by breeding ADF WT and Tg mice. Animals were screened by PCR of their tail DNA to determine their genotypes. At 8 weeks of age, male ADF WT and Tg mice (23.5–24.8 g) were transferred to a vinyl isolator established in a hazard room designed to prevent contamination from the outside environment and randomly allocated within the same genotype to housing with 6 animals per cage. A pelleted basal diet (CRF-1; Funabashi Farm, Funabashi, Japan) and tap water were provided *ad libitum* throughout the study.

Chemical

TCDD was obtained from Radian International, Cambridge Isotope Laboratories, Inc. (Andover, MA, USA; purity: 98 %). TCDD was initially dissolved in a small volume of acetone and subsequently adjusted to the concentration of 10 μg/ml in olive oil.

Experimental design

ADF WT and Tg mice were divided into vehicle controls and TCDD treatment groups, each consisting of 6 animals. After one week of acclimation, TCDD at 150 μg/kg was intraperitoneally injected once to animals of treatment groups, and the corresponding volume of olive oil was similarly injected to vehicle controls. The dosage of TCDD was selected based on previous study results that showed oxidative stress in the liver was induced by a single bolus injection to mice[21]. One day after the treatment, the animals were sacrificed by decapitation and then examined grossly. The liver and brain were then excised and their weights were measured.

The animal protocol was reviewed and approved by the Animal Care and Use Committee of the NIHS, Japan.

Morphological assessment

For histological examination, liver tissues in all animals were fixed in 10% neutral buffered formalin (pH 7.4). After routine processing, the paraffin-embedded sections were stained with hematoxylin and eosin and then examined histopathologically under a light microscope.

For electron microscopical examination, tissue specimens from the liver and cerebral cortex were respectively prepared from three animals each of the control and treatment groups of ADF WT and Tg mice. Small tissue blocks, sized 1 mm^3, were fixed with 2.5% glutaraldehyde in 0.2 M Sorenson's sodium phosphate buffer, pH 7.2, for 8 hours at 4°C. After washing with 0.1 M PBS (pH 7.4), the tissues were post-fixed with 1% osmium tetroxide for 90 minutes. After washing in 0.1 M PBS, the tissues were dehydrated with ethanol and propylene oxide and then embedded in Epon 812. Ultrathin sections were double-stained with uranyl acetate and lead citrate. The sections were examined with JEOL-1200 EX II electron microscope (JEOL, Tokyo, Japan).

Results

After one day of TCDD treatment, absolute liver weight had decreased to 71.4% of the vehicle control group in ADF WT mice and 83.2% in ADF Tg mice (data not shown).

Histologically, apoptotic liver cell debris and also focal liver cell necrosis were sparsely observed in the centrilobular areas of both TCDD-treated WT and ADF Tg mice, without showing apparent difference in the severity between genotypes (data not shown). Vehicle control animals did not show such liver cell changes in either genotype.

Electron microscopically, liver cells of the WT mice treated with TCDD exhibited a prominent decrease of cytoplasmic glycogen granules and rough endoplasmic reticula (RERs) and an increase of smooth endoplasmic reticula (SERs) (Fig. 1B). The number of mitochondria was also decreased and the remaining mitochondria showed swelling with disorganized cristae and lucent matrix. Increased fat droplets were also evident in the cytoplasm of less affected hepatocytes. On the other hand, transgene of Trx/ADF notably attenuated these morphological changes following TCDD treatment (Fig. 1C). In the cerebral cortex, neuronal cells showed a decrease in the number of RERs, ribosomes and mitochondria in WT mice treated with TCDD (Fig. 2B) but not in ADF Tg mice treated similarly with TCDD (Fig. 2C). Vehicle control animals did not show such neuronal cell changes in either genotype.

Discussion

In the present study, acute treatment with TCDD

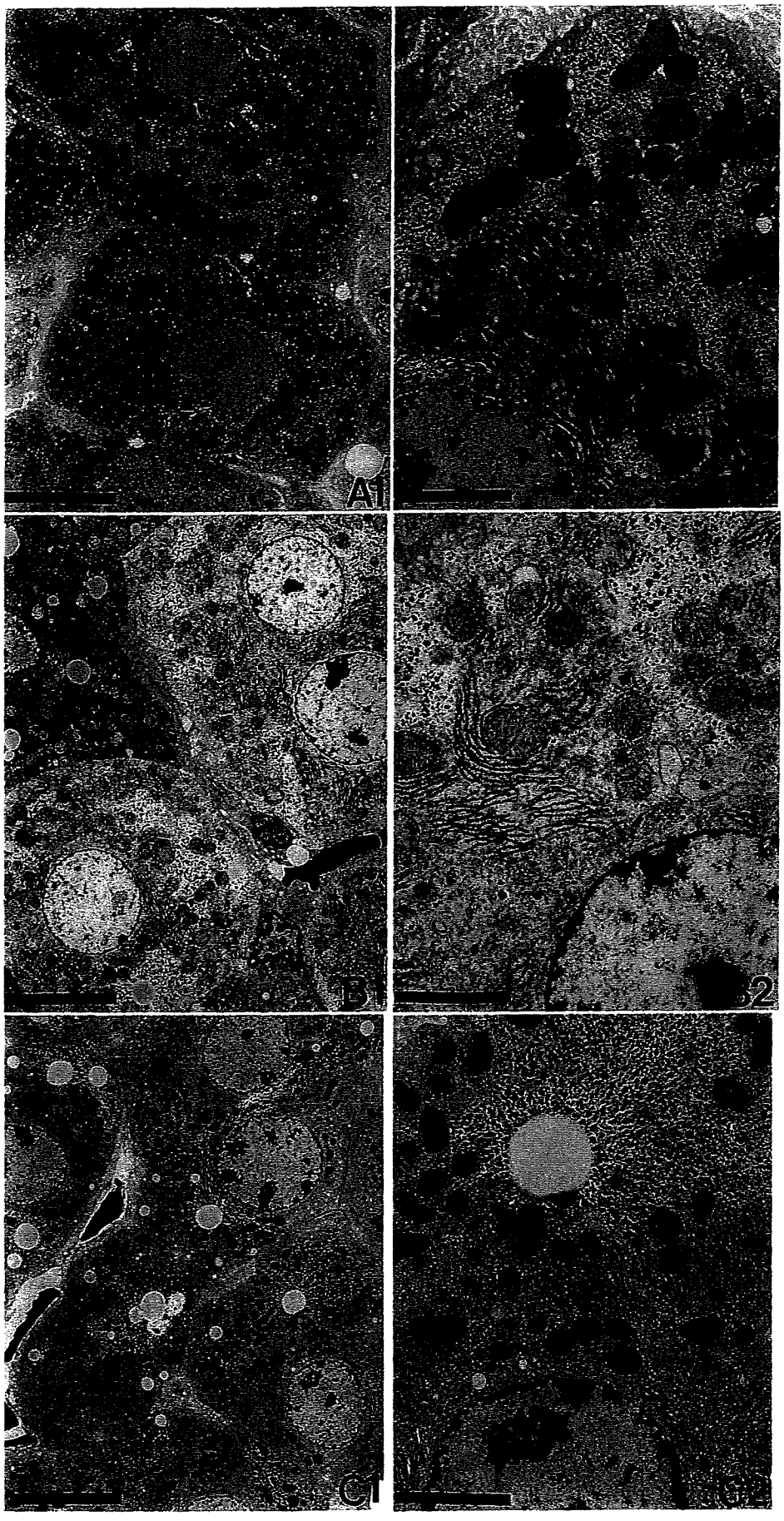

Fig. 1. Electron micrographs of liver cells from ADF WT and Tg mice treated with vehicle or TCDD. (A) Vehicle-treated ADF WT mouse, (B) TCDD-treated ADF WT mouse, and (C) TCDD-treated ADF Tg mouse. Note cytoplasmic swelling associated with a profound decrease of glycogen granules, RERs and mitochondria in the liver cells of the TCDD-treated ADF WT mouse (B). Swelling of the remaining mitochondria with disorganized cristae and lucent matrix is also evident (B). Attenuation of these morphological changes is evident in the TCDD-treated ADF Tg mouse (C). Uranyl acetate and lead citrate. Bar=10 μm (A1, B1, C1), Bar=3 μm (A2, B2, C2).

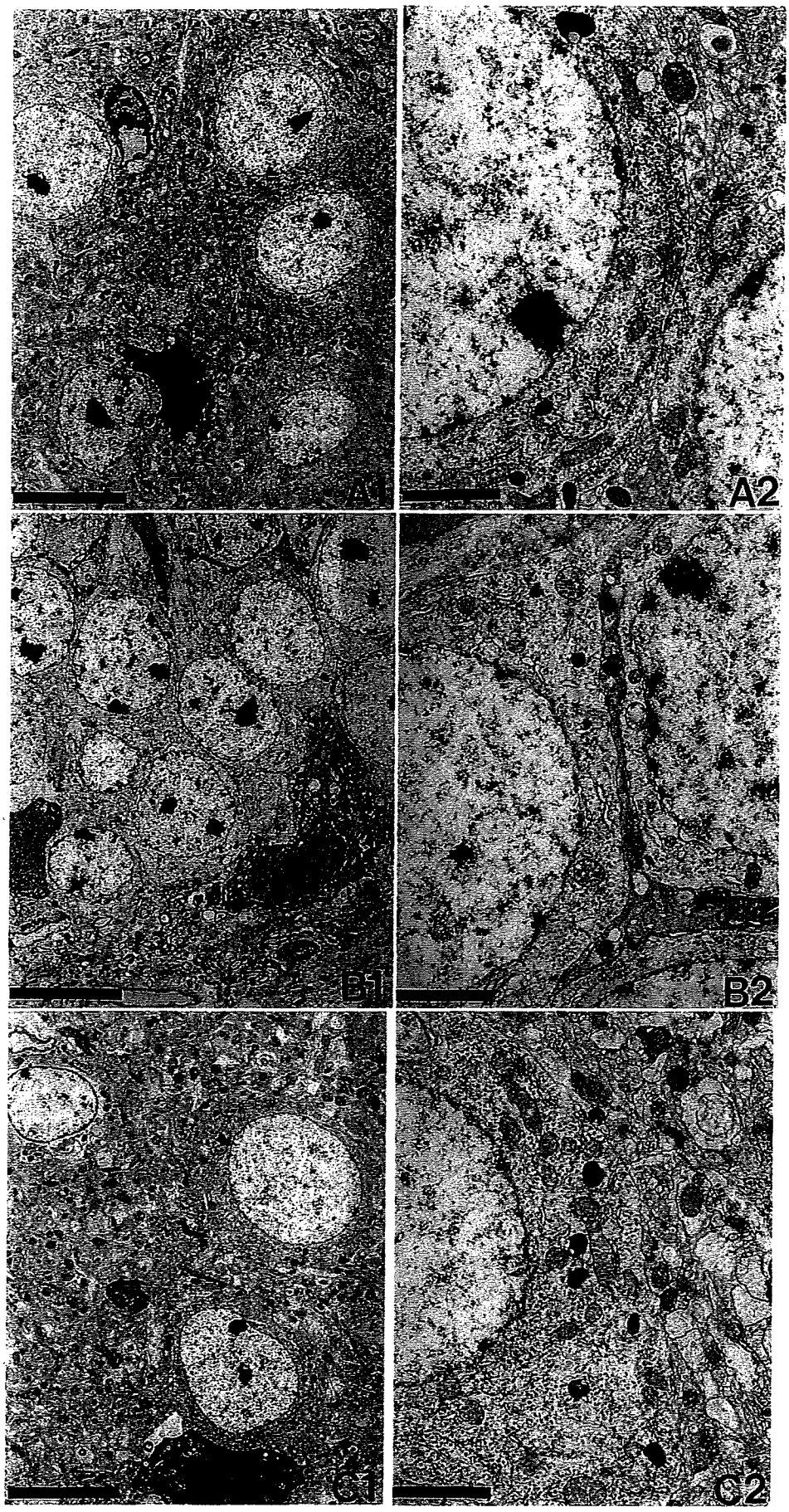

Fig. 2. Electron micrographs of neuronal cells in the cerebral cortex from ADF WT and Tg mice treated with vehicle or TCDD. (A) Vehicle-treated ADF WT mouse, (B) TCDD-treated ADF WT mouse, and (C) TCDD-treated ADF Tg mouse. Note the decrease of RER, ribosome and mitochondria in the cytoplasm of neuronal cells of the TCDD-treated ADF WT mouse (B). In the TCDD-treated ADF Tg mouse, mitochondrial swelling is also evident, but attenuation of the morphological changes can be seen, too. (C). Uranyl acetate and lead citrate. Bar=10 μm (A1, B1, C1), Bar=2 μm (A2, B2, C2).

induced ultrastructural alterations in the cytoplasmic components of liver cells characterized by prominent decrease of glycogen granules and RERs, proliferation of SERs, decrease and degradation of mitochondria, and increase of lipid droplets. These subcellular alterations were mostly consistent with those noted in the guinea pig liver following TCDD treatment[28], but concentric membrane arrays in the liver cells were not evident in the present study, presumably due to the different experimental protocol or the different species used in the studies. In the cerebral neuronal cells in the present study, alterations in subcellular components by TCDD were also evident, despite the changes being less profound than those in the liver cells. These subcellular changes in the liver and neuronal cells may represent the cytotoxic outcome of TCDD due to oxidative cellular damage and also cellular adaptation including detoxification.

Effective prevention of TCDD-induced toxicity by administration of antioxidants such as oltipraz[5-(2-pyrazinyl)-4-methyl-1,2-dithiol-3-thione] or butylated hydroxyanisole, or by pretreatment with vitamins A and E further supports the hypothesis that oxidative processes are involved in TCDD-induced toxicity[29,30]. Attenuation of subcellular changes in the liver and neuronal cells by transgene of TRX/ADF in the present study indicates the critical role of oxidative stress in the toxic events induced by TCDD, and also the protective function of ADF/TRX in these organs, as in our previous study of TCDD-induced bone marrow toxicity[26]. The protective effect of TRX/ADF against oxidative cellular damage is believed to be achieved by free radical scavengers[31], activation of DNA repair enzymes, such as activator protein endonuclease (Ref-1; redox factor-1)[32], and activation of nuclear factor-kappa B (NF-kB)[33].

Taken together, the results of our present study strongly suggest that the acute toxic effect induced in the liver and brain by a single large dose of TCDD is due to oxidative cellular damage, and that TRX/ADF plays a role in protection against TCDD-induced acute toxicity. Considering the routes and concentrations of TCDD exposed to humans, research on the effect of extremely low doses of TCDD by oral ingestion on the oxidative cellular damage of target organs is clearly warranted.

References

1. Kociba RJ, Keeler PA, Park CN, and Gehring PJ. 2,3,7,8-Tetrachlorodibenzo-*p*-dioxin (TCDD): results of a 13-week oral toxicity study in rats. Toxicol Appl Pharmacol. **35**: 553–574. 1976.
2. Chahoud I, Krowke R, Schimmel A, Merker HJ, and Neubert D. Reproductive toxicity and pharmacokinetics of 2,3,7,8-tetrachlorodibenzo-*p*-dioxin. 1. Effects of high doses on the fertility of male rats. Arch Toxicol. **63**: 432–439. 1989.
3. Funseth E and Ilbäck N-G. Effects of 2,3,7,8-tetrachlorodibenzo-*p*-dioxin on blood and spleen natural killer (NK) cell activity in the mouse. Toxicol Lett. **60**: 247–256. 1992.
4. Ivens IA, Loser E, Rinke M, Schmidt U, and Neupert M. Toxicity of 2,3,7,8-tetrachlorodibenzo-*p*-dioxin in rats after single oral administration. Toxicology. **73**: 53–69. 1992.
5. Ivens IA, Loser E, Rinke M, Schmidt U, and Mohr U. Sunchronic toxicity of 2,3,7,8-tetrachlorodibenzo-*p*-dioxin in rats. Toxicology. **83**: 181–201. 1993.
6. Erin Staples E, Murante FG, Fiore NC, Gasiewicz TA, and Silverstone AE. Thymic alteration induced by 2,3,7,8-tetrachlorodibenzo-*p*-dioxin are strictly dependent on aryl hydrocarbon receptor activation in hemopoietic cells. J Immunol. **160**: 3844–3854. 1998.
7. Poland A and Knutson JC. 2,3,7,8-Tetrachlorodibenzo-*p*-dioxin and related halogenated aromatic hydrocarbons: examination of the mechanism of toxicity. Annu Rev Pharmacol Toxicol. **22**: 517–554. 1982.
8. Cook JC, Gaido KW, and Greenlee WF. Ah receptor: relevance of mechanistic studies to human risk assessment. Environ Health Perspect. **76**: 71–77. 1987.
9. Alsarif NZ, Lawson T, and Stohs SJ. Oxidative stress induced by 2,3,7,8-tetrachlorodibenzo-*p*-dioxin is mediated by the aryl hydrocarbon (Ah) receptor complex. Toxicology. **92**: 39–51. 1994a.
10. Stohs SJ, Hassan MQ, and Murray WJ. Lipid peroxidation as a possible cause of TCDD toxicity. Biochem Biophys Res Commun. **111**: 854–859. 1983.
11. Mohammadpour H, Murray WJ, and Stohs SJ. 2,3,7,8-Tetrachlorodibenzo-*p*-dioxin -induced lipid peroxidation in genetically responsive and non-responsive mice. Arch Environ Contam Toxicol. **17**: 645–650. 1988.
12. Wahba ZZ, Lawson TA, Murray WJ, and Stohs SJ. Factors influencing the induction of DNA single strand breaks in rats by 2,3,7,8-tetrachlorodibenzo-*p*-dioxin (TCDD). Toxicology. **58**: 57–69. 1989.
13. Al-Bayati ZAF, Murray WJ, and Stohs SJ. 2,3,7,8-Tetrachlorodibenzo-*p*-dioxin-induced lipid peroxidation in hepatic and extrahepatic tissues of male and female rats. Arch Environ Contam Toxicol. **16**: 159–166. 1987.
14. Alsharif NZ, Schlueter WJ, and Stohs SJ. Stimulation of NADPH-dependent reactive oxygen species formation and DNA damage by 2,3,7,8-tetrachlorodibenzo-*p*-dioxin in rat peritoneal lavage cells. Arch Environ Contam Toxicol. **26**: 392–397. 1994b.
15. Stohs SJ. Oxidative stress induced by 2,3,7,8-tetrachlorodibenzo-*p*-dioxin (TCDD). Free Radic Biol Med. **9**: 79–90. 1990.
16. Bondy SC and Naderi S. Contribution of hepatic cytochrome P450 systems to the generation of reactive oxygen species. Biochem Pharmacol. **48**: 155–159. 1994.
17. Floyd RA. Antioxidants, oxidative stress, and degenerative neurological disorders. Proc Soc Exp Biol Med. **222**: 236–245. 1999.
18. Hassoun EA, Li F, Abushaban A, and Stohs SJ. Production of superoxide anion, lipid oxidation and DNA damage in the hepatic and brain tissues of rats after subchronic exposure to mixtures of TCDD and its congeners. J Appl Toxicol. **21**: 211–219. 2001.
19. Tritscher AM, Seacat AM, Yager JD, Groopman JD, Miller BD, Bell D, Sutter TR, and Lucier GW. Increased oxidative DNA damage in livers of 2,3,7,8-tetrachlorodibenzo-*p*-dioxin treated intact but not ovarectomized rats. Cancer Lett.

98: 219–225. 1996.
20. Hassoun EA, Wilt SC, Devito MJ, Van Birgelen A, Alsharif NZ, Birnbaum LS, and Stohs SJ. Induction of oxidative stress in brain tissues of mice after subchronic exposure to 2,3,7,8-tetrachlorodibenzo-*p*-dioxin. Toxicol Sci. **42**: 23–27. 1998.
21. Slezak BP, Hatch GE, DeVito MJ, Diliberto JJ, Slade R, Crisman K, Hassoun E, and Birnbaum LS. Oxidative stress in female B6C3F1 mice following acute and subchronic exposure to 2,3,7,8-tetrachlorodibenzo-*p*-dioxin (TCDD). Toxicol Sci. **54**: 390–398. 2000.
22. Senft AP, Dalton TP, Nebert DW, Genter MB, Hutchinson RJ, and Shertzer HG. Dioxin increases reactive oxygen production in mouse liver mitochondria. Toxicol Appl Pharmacol. **178**: 15–21. 2002.
23. Nakamura H, Nakamura K, and Yodoi J. Redox regulation of cellular activation. Annu Rev Immunol. **15**: 351–369. 1997.
24. Nakamura H, Matsuda M, Furuke K, Kitaoka Y, Iwata S, Toda K, Inamoto T, Yamaoka Y, Ozawa K, and Yodoi J. Adult T cell leukemia-derived factor/human thioredoxin protects endothelial F-2 cell injury caused by activated neutrophils or hydrogen peroxide. Immunol Lett. **42**: 75–80. 1994.
25. Yokomise H, Fukuse T, Hirata T, Ohkubo K, Go T, Muro K, Yagi K, Inui K, Hitomi S, and Mitsui A. Effect of recombinant human adult T cell leukemia-derived factor on rat lung reperfusion injury. Respiration. **61**: 99–104. 1994.
26. Yoon BI, Hirabayashi Y, Kaneko T, Kodama Y, Kanno J, Yodoi J, Kim DY, and Inoue T. Transgene expression of thioredoxin (Trx/ADF) protects against 2,3,7,8-tetrachlorodibenzo-*p*-dioxin (TCDD)-induced hematotoxicity. Arch Environ Contam Toxicol. **41**: 232–236. 2001.
27. Takagi Y, Mitsui A, Nishiyama A, Nozaki K, Sono H, Gon Y, Hashimoto N, and Yodoi J. Overexpression of thioredoxin in transgenic mice attenuates focal ischemic brain damage. Proc Natl Acad Sci USA. **96**: 4131–4136. 1999.
28. Turner JN and Collins DN. Liver morphology in guinea pigs administered either pyrolysis products of a polychlorinated biphenyl transformer fluid or 2,3,7,8-tetrachlorodibenzo-*p*-dioxin. Toxicol Appl Pharmacol. **67**: 417–429. 1983.
29. Hassan MQ, Stohs SJ, and Murray WJ. Inhibition of TCDD-induced lipid peroxidation, glutathione peroxidase activity and toxicity by BHA and glutathione. Bull Environ Contam Toxicol. **34**: 787–796. 1985.
30. Hassan MQ, Stohs SJ, and Murray WJ. Effects of vitamin E and A on TCDD-induced lipid peroxidation and other biochemical changes. Arch Environ Contam Toxicol. **14**: 437–442. 1985.
31. Tanaka T, Nishiyama Y, Okada K, Hirota K, Matsui M, Yodoi J, Hiai H, and Toyokuni S. Induction and nuclear translocation of thioredoxin by oxidative damage in the mouse kidney: independence of tubular necrosis and sulfhydryl depletion. Lab Invest. **77**: 145–155. 1997.
32. Walker LJ, Robson CN, Black E, Gillespie D, and Hickson ID. Identification of residues in the human DNA repair enzyme HAP1 (Ref-1) that are essential for redox regulation of Jun DNA binding. Mol Cell Biol. **13**: 5370–5376. 1993.
33. Schenk H, Klein M, Erdbrügger W, Dröge W, and Schulze-Osthoff K. Distinct effects of thioredoxin and antioxidants on the activation of transcription factor NF-kB and AP-1. Proc Natl Acad Sci USA. **91**: 1672–1676. 1994.

BENZENE-INDUCED HEMATOPOIETIC TOXICITY TRANSMITTED BY AHR IN THE WILD-TYPE MOUSE WAS NEGATED BY REPOPULATION OF AHR DEFICIENT BONE MARROW CELLS.

Yoko Hirabayashi[1], Byung-Il Yoon[1], Guang-Xun Li[1], Yoshiaki- Fujii-Kuriyama[2], Toyozo Kaneko[1], Jun Kanno[1], Tohru Inoue[3]

[1]Cellular and Molecular Toxicology Division, National Institute of Health Sciences
[2]Tsukuba Advanced Research Alliance (TARA), University of Tsukuba
[3]Center for Biological Safety & Research, National Institute of Health Sciences

Introduction

Recent studies have shown that the aryl hydrocarbon receptor (AhR) in primitive cells transmits negative signals for the proliferation of such cells[1, 2]. As we previously reported, primitive hemopoietic progenitor cells increases in number in AhR-knockout (KO) mice; on the other hand, relatively mature progenitor cells on the other hand, decreases in number in a homeostatic manner[1].

We have reported that benzene-induced hemopoietic toxicity is transmitted by AhR[3]. We also found that cytochrome P450 2E1 (CYP2E1) related to benzene metabolism is also up regulated in the bone marrow by benzene exposure in the bone marrow[4]. Therefore, it is of interest to hypothesize a greater role of bone marrow cells in hemopoietic toxicities rather than the hepatic metabolism. Accordingly, in the present study, benzene-induced hemopoietic toxicity was evaluated in wild type (Wt) mice after a lethal dose of whole-body irradiation followed by repopulation of bone marrow cells that lack AhR or, *vice versa,* in AhR KO mice after repopulation of Wt bone marrow cells.

As results, benzene-induced hemopoietic toxicity seems to have been transmitted through AhR, and benzene was transformed by *de novo* metabolism with CYP2E1 in the bone marrow.

Materials and Methods

Animals. The establishment of homozygous AhR KO ($AhR^{-/-}$) mice, the 129/SvJ strain, is described elsewhere[3, 5]. The breeding of heterozygous AhR KO ($AhR^{+/-}$) males with $AhR^{+/-}$ females generated wild-type ($AhR^{+/+}$), $AhR^{+/-}$, and $AhR^{-/-}$mice. The neonates were genotyped by PCR screening of DNA from the tail. Female mice (12 weeks old) were used in the study. Eight-week-old C57BL/6 male mice from Japan SLC (Shizuoka, Japan) were used as recipients for the repopulation assay and the assay of CFU in the spleen. All the mice were housed under specific pathogen-free conditions at 24 ± 1°C and 55 ± 10%, using a 12-hr light-dark cycle. Autoclaved tap water and food pellets were provided *ad libitum.*

Blood and bone marrow (BM) parameters. Peripheral blood was collected from the orbital sinus. Peripheral blood leukocyte (WBC), red blood cell (RBC) and platelet (PLT) counts were determined using a blood cell counter (Sysmex M-2000, Sysmex Co., Kobe, Japan). Bone marrow (BM) cellularity was evaluated by harvesting BM cells from the femurs of each mouse[6]. The animals were sacrificed. Then a 27-gauge needle was inserted into the femoral bone cavity through the proximal and distal edges of the bone shafts, and BM cells were flushed out under pressure by injecting 2 ml of a-MEM. A single-cell suspension was obtained by gently triturating the BM cells through the 27-gauge needle, and cells were counted using Sysmex M-2000.

Irradiation. Recipient mice were exposed to a lethal radiation of 800.1 cGy, at a dose rate of 124 cGy/min, using a ^{137}Cs-gamma irradiator (Gamma Cell 40, CSR, Toronto, Canada) with a 0.5-mm aluminum-copper filter.

CFU-S Assay. The Till and McCulloch method[7]was used to determine the number of colony-forming units in the

spleen (CFU-S). Aliquots of BM cell suspensions were used to evaluate the number of CFU-S. The number of BM cells was adjusted to that appropriate for producing nonconfluent spleen colonies, and the cells were then transplanted into lethally irradiated mice by injection through the tail vein. Spleens were harvested 9 and 13 days after the injection, and fixed in Bouin's solution. Macroscopic spleen colonies were counted under an inversion microscope at a magnification of x 5.6.

CFU-GM and CFU-E Assay. *in vitro* colony formation was assayed in semisolid methylcellulose culture[6, 8]. Briefly, 8 x 10^4 BM cells suspended in 100 ml of medium were added to 3.9 ml of a culture medium containing 0.8% methyl cellulose, 30% fetal calf serum, 1% bovine serum albumin, 10^{-4} M 2-mercaptoethanol, with 10 ng/ml murine granulocyte-macrophage colony-stimulating factor (GM-CSF) for CFU-GM or 1ng/ml murine Interleukin-3 and 2 U/ml erythro-poietin for erythroid CFU (CFU-E). One-ml aliquots containing 2 x 10^4 BM cells were plated in triplicate in a 35-mm tissue-culture plate, and incubated for six days in a completely humidified incubator at 37 °C with 5% CO_2 in air. Colonies were counted under an inverted microscope at magnifications of x 40 for CFU-GM after 6-day culture and x100 for CFU-E after 3-day culture.

***BM repopulation assay*[9].** The BM repopulation assay was performed similarly to the assay of CFU-S, except that 10^6 BM cells were injected into lethally irradiated mice. One month after the transfusion of BM cells, the repopulated mice were used in the experiment.

Results and Discussion

As previously reported, AhR-KO mouse showed a significant increase in WBC counts (**Figure 1** A). This was also consistent with the high number of myeloid progenitor cells, *i.e.*, CFU-S-9 and CFU-S-13, observed in the AhR-KO mice (**Figure 1**, B). Thus, steady-state hemopoiesis is presumed to be suppressed by AhR signaling due to the possible presence of a physiological ligand, which is not readily observed in AhR-KO mice. In response to such an AhR-null effect, the AhR-KO mouse reversely shows extensive hemopoiesis in the spleen, although this hemopoietic enhancement is also reflected in another negative hemopoietic regulation in the BM. Accordingly, in the present study, benzene-induced hematotoxicity was evaluated in the Wt mice after a lethal dose of whole-body irradiation followed by the repopulation of BM cells that lack AhR.

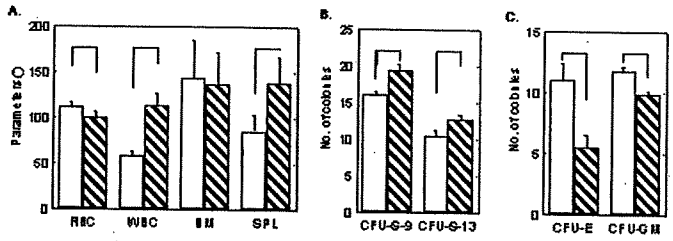

Figure 1: Comparison of various blood parameters between Wt mice (open columns) and AhR-KO mice (shaded columns) [1]; **A.** Peripheral blood, bone marrow and spleen weight. * Parameters indicate the counts of peripheral red blood cells (RBCs, $\times 10^8$/ml) and white blood cells (WBCs, $\times 10^6$/ml), bone marrow cellularity (BM, $\times 10^5$/femur), and weight of spleen (SPL, mg). **B.** Number of colony-forming units in spleen (CFU-S/1×10^5 BM cells) observed on days 9 (CFU-S-9) and 13 (CFU-S-13). **C.** Numbers of *in vitro* granulocyte-macrophage CFUs (CFU-GM/5×10^3 BM cells) and erythroid CFU (CFU-E/1×10^4 BM cells). †: Significant difference between Wt and AhR-KO mice determined by *t*-test at $p<0.05$.

Figures 2, A-C, show the RBC (A), WBC (B), and platelet (PLT: C) counts (per mL) in the peripheral blood after repopulation of the BM. In each figure, in the Wt mice repopulated with Wt BM cells (two columns on the left), the groups subjected to intraperitoneal benzene exposure (second from the left) show significant decreases in RBC and PLT counts (92% and 69%; p=0.010 and 0.016, respectively) compared with the sham exposure groups (farthest left in each figure), except 2B, i.e., WBC counts (96%). When the mice repopulated with AhR-KO BM cells (two columns on the right) are exposed to benzene, there are no significant differences between the sham exposure groups (second from the right) and the benzene exposed groups (farthest right) in A through C. Significant decreases

observed in the Wt mice repopulated with Wt BM cells were negated when the Wt mice were repopulated with AhR-KO BM cells; thus, the reduction in the number of peripheral blood cells observed in the Wt mice after benzene exposure is assumed to be responsible for the AhR expression in BM cells. Although the two sham exposures (i.e., Wt mice, open column; and AhR-KO mice, solid column) are essentially identical in A and C, there seems to be insufficient recovery of the BM in transplantation in Figure 2B, and the solid column is significantly reduced (see, Figure 3 on CFU-GM).

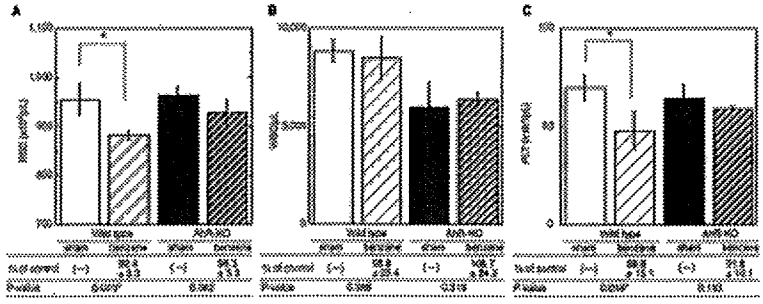

Figure 2: Comparison of various blood parameters in peripheral blood; A, RBC, B, WBC, and C, platelets (open bars vs lightly shaded bars in Wt mice repopulated with Wt BM cells; solid bars vs heavily shaded bars in Wt mice repopulated with AhR BM cells).

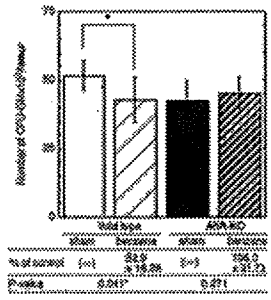

Figure 3: *: Significant difference between sham and exposed determined by *t*-test at $p<0.05$.

In Figure 3, again, the significant decrease in the number of granulocyte-macrophage colony-forming units *in vitro* (CFU- GM/5 x10^3 BM cells) in the BM cells from the Wt mice repopulated with Wt BM cells (82.9% in benzene exposure, lightly shaded column to the right of the sham exposure, open leftmost column; p=0.041) is negated in the BM cells from mice repopulated with AhR-KO BM cells (sham exposure, solid column; and benzene exposure, heavily shaded column, respectively). In this figure, the efficiency of repopulation with AhR- KO BM cells (solid column) seems to be insufficient, since the solid column is smaller than the open column (p=0.025). The mechanism underling the incomplete recovery of AhR-KO BM cells, is still unknown; however, the sublethal irradiation of the recipient mice may be the case, where suppressive intrinsic factors may have been released from tissues given the lethal dose of irradiation received by the host animals.

Despite the insufficient recovery of the number of GM-CFU in mice repopulated with AhR-KO BM cells, number of BM cells, regardless of repopulated cell type (either Wt or AhR-KO BM cells) and type of exposure (either benzene or sham exposure), there were no significant differences in number of BM cells among the groups in a homeostatic manner (**Figure 4**, A; 91.4% and 92.4%, respectively, p>0.1). However, after benzene exposure, a significant decrease in splenic weight was observed in the Wt→Wt group (85.0%, p=0.022), but not in the AhR-KO-BM→Wt group (90.0%, p=0.173). This supports the notion that AhR-KO negates the suppressive effect on splenic weight after benzene exposure.

Figure 4: Comparison of number of BM cells (A) or weight of spleen (B) with or without benzene exposure, in mice repopulated with Wt BM cells or in mice repopulated with AhR-KO BM cells. (Wt mice repopulated with Wt BM cells, lightly shaded columns, second from left; or without benzene exposure, open columns, farthest left, benzene exposure vs Wt mice repopulated with AhR-KO BM cells, each of the two right columns).

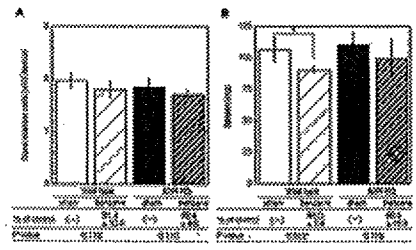

Conclusions

The up-regulation of CYP2E1 after benzene exposure was specifically observed in our previous microarray study of the bone marrow tissue[4]. The analysis of the gene expression specifically derived from the hematopoietic stem cell compartment[10], and the evaluation of the toxicological alteration of such an expression as a measure of stem cell specific toxicological biomarkers are hot issues in the current hematotoxicology[11]. Mice that have been lethally irradiated and repopulated with BM cells from AhR-KO mice essentially did not shown any benzene-induced hematotoxicity, implying that such toxicity is derived from *de novo* metabolisms with CYP2E1 in the BM other than hepatic metabolism. The present study raises two questions on AhR-mediated TCDD-induced hematotoxicity: Do Wt mice repopulated with AhR-KO BM cells show hematotoxicity by TCDD unlike in the case of benzene exposure? If such is the case, what would be the transmitter from the site of xenobiotic metabolic activation to the bone marrow?

References

1 Hirabayashi, Y., Li, G., Yoon, B.I., Fujii-Kuriyama, Y., Kaneko, T., Kanno, J., and Inoue, T. (2003) Organohalogen Compounds, 64, 270

2 Garrett, R.W., and Gasiewicz, T.A. (2005) Meeting abstract [Molecular Regulation of Stem Cell, Keystone symosia], 61

3 Yoon, B.I., Hirabayashi, Y., Kawasaki, Y., Kodama, Y., Kaneko, T., Kanno, J., Kim, D.Y., Fujii-Kuriyama, Y., and Inoue, T. (2002) Toxicol Sci, 70, 150

4 Yoon, B.I., Li, G.X., Kitada, K., Kawasaki, Y., Igarashi, K., Kodama, Y., Inoue, T., Kobayashi, K., Kanno, J., Kim, D.Y., Inoue, T., and Hirabayashi, Y. (2003) Environ Health Perspect, 111, 1411

5 Mimura, J., Yamashita, K., Nakamura, K., Morita, M., Takagi, T.N., Nakao, K., Ema, M., Sogawa, K., Yasuda, M., Katsuki, M., and Fujii-Kuriyama, Y. (1997) Genes Cells, 2, 645

6 Yoon, B.I., Hirabayashi, Y., Kawasaki, Y., Kodama, Y., Kaneko, T., Kim, D.Y., and Inoue, T. (2001) Exp Hematol, 29, 278

7 Till, J.E., and McCulloch, E.A. (1961) Radiat Res, 14, 213

8 Hirabayashi, Y., Matsuda, M., Aizawa, S., Kodama, Y., Kanno, J., and Inoue, T. (2002) Exp Biol Med (Maywood), 227, 474

9 Hirabayashi, Y., Inoue, T., Suda, Y., Aizawa, S., Ikawa, Y., and Kanisawa, M. (1992) Exp Hematol, 20, 167

10 Ivanova, N.B., Dimos, J.T., Schaniel, C., Hackney, J.A., Moore, K.A., and Lemischka, I.R. (2002) Science, 298, 601

11 Hirabayashi, Y., Inoue, T. (2005) in: Handbook of Toxicogenomics (Borlak J., Ed.), Wiley-VCH Verlag GMbH & Co. Weinheim, 583.

医学のあゆみ Vol.213 No.4 2005 4 23

あゆみ

環境生体応答——Toxicogenomics

フォーラム

はじめに
Introduction

井上　達
Tohru INOUE
国立医薬品食品衛生研究所

解読された全ゲノムの塩基配列を利用して明らかにしうることは，ゲノム構造に拘束された決定論的な生命の枠組みと，遺伝子発現の可塑性によって展開する確率論的な生命の多様性である．前者ではミレニウム計画などで傾注された薬物代謝における SNPs の発見やテーラーメイド創薬戦略の研究が進んだ一方，後者でいまゲノムと環境の相互作用によって展開される生物の多様なエピジェネティクスとしての環境生体応答学がおもしろくなっている[1]．トキシコゲノミクス[2]はどちらかといえば後者に属し，それはトランスクリプトミクスやプロテオミクス，インフォマティクスなどの総体によって描きだされるトキシコパノミクス(toxicopanomics)とでもよぶべき新領域である．

トキシコパノミクスは物質と生体の応答学であるが，生体側からみる手法をトランスクリプトミクスと考えれば，生体内生成物の側からみる解析手法は主としてプロテオミクスによる．前者では DNA チップなどの高密度集積アレイ解析を用い，後者では GC マスなどの蛋白定量解析手技を適用する．ちなみに代謝に注目すると，前者は，メタボノミクス的手法，後者では代謝物に焦点をあてたメタボロミクスを中心に探査することになる．

この世界ではゲノム科学が取り組んできた帰納的解析にとどまらず，遺伝子発現や蛋白発現をフェノタイプとして用いることによって演繹的に後生的な予測が可能となる．オミクス領域を積極的にそうした予測のツールに発展させようとする点に，ここで取り上げるトキシコパノミクスの，決定論的な応用としての“マイクロアレイ診断”と異なった特徴がある．遺伝子発現情報は塩基配列情報にとどまり転写の経路や蛋白がフェノタイプとしてもつ情報の多様性(complexity)をカバーしないから予測は限定的になる．エピジェネティクスに対する予測能は未知である．そうした限界にもかかわらずこのものの生命の安全性や環境科学へ果たす役割には大きな期待が寄せられている．

文献

1) 井上　達：毒性学の現状と展望—あたらしいバイオサイエンスとしての生体異物応答科学．科学，**74**(1)：18-23，2004.
2) Inoue, T. and Pennie, W. D.(ed.)：Toxicogenomics. Springer-Verlag, Tokyo, 2003, pp.1-11.

The Journal of Toxicological Sciences,
Vol.31, No. 1, 35-47, 2006

SEMI-QUANTITATIVE IMMUNOHISTOCHEMICAL ANALYSIS OF MALE RAT-SPECIFIC α_{2u}-GLOBULIN ACCUMULATION FOR CHEMICAL TOXICITY EVALUATION

Masao HAMAMURA[1], Akihiko HIROSE[2], Eiichi KAMATA[2], Koshiro KATOKU[1], Emiko KUWASAKI[1], Takafumi OSHIKATA[1], Yutaka NAKAHARA[1], Makoto EMA[2] and Ryuichi HASEGAWA[2]

[1]Panapharm Laboratories Co., Ltd.,
1285 Kurisaki-machi, Uto-shi, Kumamoto 869-0425, Japan
[2]National Institute of Health Sciences,
1-18-1 Kamiyoga, Setagaya-ku, Tokyo 158-8501, Japan

(Received August 8, 2005; Accepted October 31, 2005)

ABSTRACT — We purified male rat urinary α_{2u}-globulin, prepared the antibody in rabbits, and improved an immunohistochemical detection method using this antibody for male rat-specific α_{2u}-globulin accumulation appearing as hyaline droplets in the kidneys. Our prepared antibody reacted specifically with α_{2u}-globulin in both immunohistochemical and Western blotting analyses, furthermore, and the graded immuno-reactivities on the slide were well associated with computational image analyzing results. Using this method, we retrospectively analyzed the renal sections from the toxicity studies of 12 nephrotoxic chemicals, which had already been conducted under the Japanese Existing Chemicals Survey Program. We demonstrated that the hyaline droplets induced by treatment with 10 chemicals (1,4-dibromobenzene, dicyclopentadiene, 3,4-dimethylaniline, 1,4-dicyanobenzene, tetrahydrothiophene-1,1-dioxide, 1,3-dicyanobenzene, acenaphthene, 3,4-dichloro-1-butene, 3a,4,7,7a-tetrahydro-1H-indene and 3,5,5-trimethylhexan-1-ol) were directly associated with α_{2u}-globulin accumulation. This immunohistochemical method is convenient for applying, even retrospectively, paraffin sections from general toxicity studies and could be useful for qualifying male rat-specific hyaline droplets consisting of α_{2u}-globulin and renal risk in humans.

KEY WORDS: α_{2u}-globulin, Immunohistochemistry, Hyaline droplet, Nephrotoxicity

INTRODUCTION

For risk assessment of chemicals, the most critical data are derived from animal toxicity studies because of a general lack of information on humans. Although all available results from animal studies have been applied to human risk assessment, in principle, exclusion of some specific toxicities, which might not occur in humans, should be taken into account. Among laboratory animals, the rat has been commonly used for toxicity studies, especially sub-acute, long-term or carcinogenicity studies. Nephropathy with hyaline droplets and renal tubular neoplasia caused by chemicals inducing α_{2u}-globulin accumulation (CIGA) are considered to be a male rat-specific toxicity, not occurring in female rats or other animals, including primates. Although low molecular proteins homologous to α_{2u}-globulin can be detected in other species, including mice and humans, none of these proteins have been confirmed to bind to CIGA, followed by accumulation of the protein-CIGA complex as in the case of α_{2u}-globulin. It is therefore believed that renal toxicity induced by CIGA in male rats is unlikely to occur in humans (Hard *et al.*, 1993).

α_{2u}-Globulin was first identified in male rat urine (Roy and Neuhaus, 1966), and had been reported to be a male rat-specific protein with a molecular weight of 18 to 20 kDa. The major source of urinary α_{2u}-globulin

Correspondence: Masao HAMAMURA (E-mail: hamamura@panapharm.co.jp)

is the liver, where α_{2u}-globulin mRNA constitutes approximately 1% of the total hepatic mRNA (Sippel *et al.*, 1976; Kurtz and Feigelson, 1977). Neither α_{2u}-globulin nor its mRNA is detectable in the female liver (Sippel *et al.*, 1975, 1976; MacInnes *et al.*, 1986). The blood α_{2u}-globulin secreted from the liver is freely filtered through the glomerulus, and in mature rats, about two-thirds of the filtered protein is reabsorbed by tubules and the remainder is excreted through the urine (Neuhaus *et al.*, 1981). CIGA binds noncovalently to α_{2u}-globulin, and the resulting complex shows less degradability with proteolytic enzymes, causing an accumulation of the complex that is detectable as hyaline droplets with a light microscope. Various chemicals have been suspected of being CIGA based on detection of the evidence for exacerbation of hyaline droplets in renal proximal tubules in male rats, though not in females. Direct evidence for increasing α_{2u}-globulin levels has been demonstrated for only a few of these chemicals, however, including 2,2,4-trimethylpentane (Stonard *et al.*, 1986; Charbonneau *et al.*, 1987; Lock *et al.*, 1987), decalin (Kanerva *et al.*, 1987), d-limonene (Lehman-McKeeman *et al.*, 1989; Webb *et al.*, 1989), 1,4-dichlorobenzene (Charbonneau *et al.*, 1989), isophorone (Strasser *et al.*, 1988), lindane (Dietrich and Swenberg, 1990), tri- or per-chloroethylene and pentachoroethane (Goldsworthy *et al.*, 1888).

A number of initial safety assessments has so far been conducted for industrial chemicals, including both new and existing chemicals by the Japanese government or the OECD high production volume chemicals programs. Certain chemicals among these industrial chemicals have been suspected of being CIGA. In some cases, however, renal changes in male rats have been assessed as the endpoint for extrapolation to human health risk owing to a lack of direct evidence caused by α_{2u}-globulin accumulation, because no antibody against α_{2u}-globulin is commercially available for general toxicity studies. Some immunohistochemical α_{2u}-globulin analysis methods had already been developed (Burnett *et al.*, 1989; Hashimoto and Takaya, 1992; Caldwell *et al.*, 1999). As these methods required glycolmethacrylate embedding or specific computational analysis, they would be inappropriate for confirming α_{2u}-globulin accumulation in routinely conducted guideline-based toxicity studies. We therefore improved an immunohistochemical α_{2u}-globulin detection system using paraffin sections, which are generally used for standard toxicity studies. We evaluated the several chemicals suspected of being CIGA, moreover, and indicated the direct evidence caused by α_{2u}-globulin accumulation.

MATERIALS AND METHODS

Preparation of anti α_{2u}-globulin antibody

α_{2u}-globulin as an antigen was obtained from the urine collected from aged male rats, pooled, and used to immunize rabbits. The immunization procedures, including the amount of antigen and immunizing intervals, were determined from the results of a preliminary test referring to the methods of Kurtz *et al.* (1976). The antigen was injected under the skin at a dose of 1 mg/animal (1st injection) or 0.5 mg/animal (2nd and subsequent injections) once at two weeks. Blood sampling was conducted periodically and the antibody titer measured. When the antibody titer level reached a plateau, whole blood was collected and antiserum was obtained from the blood. The antiserum was used for immunohistochemistry and immuno-electron microscopy. For measurement of the α_{2u}-globulin content in the urine and tissues, the antibody was purified from the antiserum using a DEAE ionic exchange column after ammonium sulfate precipitation. The singularity of the antibody was confirmed as a single diffuse band of approximately 19 kDa by Western blotting analysis. This study and the following study were carried out in accordance with the Law for the Humane Treatment and Management of Animals and the Standards Relating to the Care and Management, etc. of Experimental Animals in Japan.

Experiment 1 Confirmation of specific reactivity of the antibody to α_{2u}-globulin

1. Preparation of α_{2u}-globulin nephropathy rats

To confirm the specific reactivity of the anti-α_{2u}-globulin antibody, we prepared α_{2u}-globulin nephropathy rats as follows. Male and female Crj:CD(SD)IGS rats were obtained from Charles River Japan Inc. and used at the age of 11 weeks. d-Limonene (Nacalai Tesque Inc.), a well-known α_{2u}-globulin nephropathy inducer, was administered to the rats, consisting of 4 males and 4 females each, for 10 days at doses of 0, 150 and 300 mg/kg/day by gavage using corn oil as a vehicle. The rats were housed individually in stainless steel wire cages in an animal room with a controlled temperature of 24±2°C, humidity of 55±10% and a 12-hr light/dark cycle (lighting from 7:00 to 19:00) and allowed access to food and water ad libitum.

Pooled urine was collected for 24 hr on the day before the start of administration and on Day 9 of administration. After the 10-day administration period,